2001-01-4063

An Evaluation of Elber-Type Crack Retardation Models

Marco Antonio Meggiolaro
Jaime Tupiassú Pinho de Castro
Mechanical Engineering Department
Pontifical Catholic University of Rio de Janeiro (PUC-Rio), Brazil
e-mails: meggi@mec.puc-rio.br, jtcastro@mec.puc-rio.br

ABSTRACT

In this work, a review of plasticity induced crack closure is presented, along with models proposed to quantify its effect on the subsequent crack growth rate. The stress state dependence of crack closure is discussed. Overload-induced retardation effects on the crack growth rate are considered, based on the crack closure idea, and improvements to the traditional models are proposed to account for crack arrest and crack acceleration after compressive underloads. Using a general-purpose fatigue design program, the models and the proposed modifications are compared with experimental results from various load spectra, and with simulated histories illustrating their main features.

Keywords: Fatigue, Crack Propagation, Sequence Effects, Retardation Models, Complex Loading.

INTRODUCTION

Load interaction models must be accounted for to accurately predict fatigue crack propagation life under complex loading. Tensile overloads, when applied over a constant amplitude loading, can retard or even arrest the subsequent crack growth, and compressive underloads can also affect the rate of crack propagation [1-3], see Figure 1.

Neglecting these effects in fatigue life calculations under complex loading can completely invalidate the predictions. However, the generation of a universal algorithm to quantify these effects for design purposes is particularly difficult, due to the number and to the complexity of the mechanisms involved in crack retardation, among them

- plasticity-induced crack closure;
- blunting and/or bifurcation of the crack tip;
- residual stresses and/or strains;
- strain-hardening or strain induced phase transformation;
- crack face roughness; and
- oxidation of the crack faces.

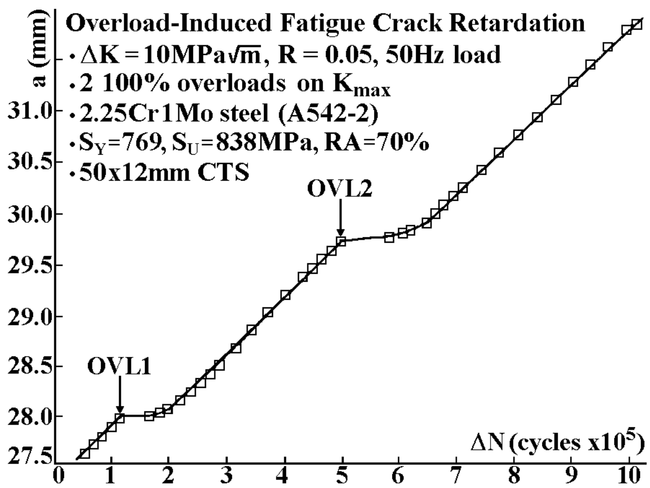

Figure 1. Fatigue crack growth retardation induced by tensile overloads [3].

The detailed discussion of this complex phenomenology is considered beyond the scope of this work (a revision of the phenomenological problem can be found in [1]). Moreover, the relative importance of the several mechanisms can vary from case to case.

On the other hand, the principal characteristic of fatigue cracks is to propagate cutting a material that has already been deformed by the plastic zone that always accompanies their tips. Therefore, fatigue crack faces are always embedded in an envelope of (plastic) residual strains and, consequently, they compress their faces when completely discharged, and open alleviating in a progressive way the (compressive) load transmitted through them.

In the early seventies, Elber [4] discovered that fatigue cracks opened gradually, remaining partially closed for loads substantially higher than zero. This was attributed to the compressive loads transmitted through the faces of an unloaded fatigue crack, caused by the plastic strains that surround it, a phenomenon termed ***plasticity-induced fatigue crack closure***.

CRACK CLOSURE – Elber was one of the first to attempt to describe, with the aid of a physical model, the connection between load sequence, plastic deformation (by way of crack closure) and crack growth rate. He assumed that crack growth cannot take place under cyclic loads until the fatigue crack is fully opened. According to him, only after the load completely opened the crack at a stress intensity factor $\mathbf{K_{op} > 0}$, would the crack tip be stressed. Therefore, the bigger the $\mathbf{K_{op}}$, the less would be the ***effective*** stress intensity range $\mathbf{\Delta K_{eff} = K_{max} - K_{op}}$, and this $\mathbf{\Delta K_{eff}}$ instead of the range $\mathbf{\Delta K = K_{max} - K_{min}}$ would be the fatigue crack propagation rate controlling parameter. Based on experiments on 2024-T3 aluminum, Elber proposed a modification to the Paris growth rule by using this effective stress intensity range to calculate the crack propagation under constant amplitude loads

$$\frac{da}{dN} = A \cdot (\Delta K_{eff})^m = A \cdot \left(\frac{\Delta K - \Delta K_{th}}{1-R} \right)^m \tag{1}$$

where $\mathbf{da/dN}$ is the fatigue crack growth rate, $\mathbf{R=K_{min}/K_{max}}$ is the stress ratio, $\mathbf{\Delta K_{th}}$ is the propagation threshold, and $\mathbf{A}$ and $\mathbf{m}$ are material properties, which should be experimentally measured. The threshold stress intensity factor range used in this model can be determined for any positive stress ratio $\mathbf{R > 0}$ by, for instance

$$\Delta K_{th} = (1 - \alpha_t R)\, \Delta K_0 \tag{2}$$

where $\mathbf{\Delta K_0}$ is the crack propagation threshold value of the stress intensity factor range obtained from $\mathbf{R = 0}$ constant amplitude tests, and $\mathbf{\alpha_t}$ is a material constant determined from constant-amplitude test data for various stress ratios.

Newman [5] found that crack closure does not only depend on $\mathbf{R}$, as proposed by Elber, but is also dependent on the maximum stress level $\mathbf{\sigma_{max}}$. According to Newman, the crack opening stress intensity factor can be calculated from the closure function $\mathbf{f}$

$$f = \frac{K_{op}}{K_{max}} = \begin{cases} \max(R, A_0 + A_1 R + A_2 R^2 + A_3 R^3), & R \ge 0 \\ A_0 + A_1 R, & -2 \le R < 0 \end{cases} \tag{3}$$

where the polynomial coefficients are given by

$$\begin{cases} A_0 = (0.825 - 0.34\alpha + 0.05\alpha^2) \cdot [\cos(\pi\sigma_{max} / 2S_{fl})]^{1/\alpha} \\ A_1 = (0.415 - 0.071\alpha) \cdot \sigma_{max} / S_{fl} \\ A_2 = 1 - A_0 - A_1 - A_3 \\ A_3 = 2A_0 + A_1 - 1 \end{cases} \tag{4}$$

where $\mathbf{\sigma_{max}}$ is the maximum applied stress, $\mathbf{S_{fl}}$ is the material flow strength (for convenience defined as the average between the material yielding and ultimate strengths, $\mathbf{S_{fl} = (S_Y + S_U)/2}$), and $\boldsymbol{\alpha}$ is a plane stress/strain constraint factor, with values ranging from $\boldsymbol{\alpha} = \mathbf{1}$ for plane stress to up to $\boldsymbol{\alpha} = \mathbf{3}$ for plane strain.

From the definition of Newman's closure function $\mathbf{f}$, the effective stress intensity range $\mathbf{\Delta K_{eff} = K_{max} - K_{op}}$ can be rewritten as

$$\Delta K_{eff} = (1-f) \cdot K_{max} = \frac{1-f}{1-R} \Delta K \tag{5}$$

Based on the above expression for the effective stress intensity range, Forman et al. [6] proposed the following fatigue crack propagation rule to model all three crack growth regimes [1-3], including the effect of the stress state through Newman's closure function

$$\frac{da}{dN} = A \cdot \left(\frac{1-f}{1-R} \Delta K \right)^m \frac{(1 - \Delta K_{th}/\Delta K)^p}{(1 - K_{max}/K_C)^q} \tag{6}$$

where $\mathbf{K_C}$ is the critical (rupture) stress intensity factor, $\mathbf{A}$, $\mathbf{m}$, $\mathbf{p}$, and $\mathbf{q}$ are experimentally adjustable constants, and $\mathbf{\Delta K_{th}}$ can be calculated using equation (2).

Assuming that the fatigue crack growth rate is ***controlled*** by $\mathbf{\Delta K_{eff}}$ instead of by $\mathbf{\Delta K}$ (and, therefore, that plasticity induced closure is the ***sole*** mechanism which affects the propagation process), the need for taking into account the stress state in fatigue crack propagation tests must be emphasized. Consider, for instance, the effective stress intensity range $\mathbf{\Delta K_{eff}}$ predicted by Newman for the ***plane stress*** case ($\boldsymbol{\alpha} = \mathbf{1}$) when $\mathbf{R = 0}$. From equations (3-5), $\mathbf{\Delta K_{eff}}$ is approximately equal to ***half*** the value of $\mathbf{\Delta K}$. This means that $\mathbf{da/dN}$ curves experimentally fitted to $\mathbf{\Delta K}$ values without considering the crack closure effect would be actually correlating the measured $\mathbf{da/dN}$ rates with ***twice*** the actual (effective) stress intensity range acting on the crack tip. On the other hand, $\mathbf{da/dN}$ curves obtained in the same way ($\mathbf{R = 0}$) under ***plane strain*** conditions ($\boldsymbol{\alpha} = \mathbf{3}$) would be actually correlating $\mathbf{da/dN}$ with approximately **4/3** of (and ***not twice***) the effective stress intensity range. Therefore, one could not indiscriminately use crack growth equation constants obtained under a certain stress condition (e.g. plane stress) to predict crack growth under a different state (e.g. plane strain), even under the same stress ratio $\mathbf{R}$.

E.g., if a Paris $\mathbf{da/dN}$ vs. $\mathbf{\Delta K}$ equation with exponent $\mathbf{m = 3.0}$, measured under plane stress conditions and $\mathbf{R = 0}$, is used to predict crack propagation under plane strain, the predicted crack growth rate would be $\mathbf{[(4/3)/2]^m \approx 0.3}$ times the actual rate, a ***non-conservative error of* 70%**. Therefore, to avoid this (unacceptable) error, it would be necessary to convert the measured crack growth constants associated with one stress condition to the other using appropriate crack closure functions. Another approach would be to use in the predictions only $\mathbf{da/dN}$ vs. $\mathbf{\Delta K}$ rules such as equation

(6), that already have embedded the stress state dependent closure functions.

This alarming prediction implies that the usual practice of plotting **da/dN** vs. **ΔK** instead of **da/dN** vs. **ΔK_{eff}** to describe fatigue crack growth tests would be highly inappropriate, because **da/dN** would also be a strong function of the specimen thickness **t**, which controls the dominant stress state at the crack tip (assuming that the classical ASTM E399 requirements for validating a **K_{IC}** toughness test could also be used in fatigue crack growth, plane strain conditions would apply if **$t > 2.5[K_{max}/S_Y]^2$**). In other words, one could expect to measure quite different **da/dN** fatigue crack growth rates when testing thin or thick specimens of a given material under the same **ΔK** and **R** conditions. Moreover, the concept of a "thin" or "thick" specimen would also depend on the load, since **K_{max}** increases with the applied stress. However, this thickness effect on **da/dN** is not recognized by the ASTM E645 standard on the measurement of fatigue crack propagation, which, in spite of mentioning the importance of crack closure, only requires specimens sufficiently thick to avoid buckling during the tests.

The errors associated with plotting **da/dN** vs. **ΔK** instead of **ΔK_{eff}** to predict crack growth under different stress states can be illustrated e.g. using **$m = 3.25$** for the exponent of the Paris equation of an aluminum alloy. If data is measured under plane stress conditions without considering crack closure, then the prediction under plane strain would be **$(\Delta K_{eff,\ \sigma}/\Delta K_{eff,\ \varepsilon})^m$** times the actual rate, a ***non-conservative*** error of **$[1 - (\Delta K_{eff,\ \sigma}/\Delta K_{eff,\ \varepsilon})^{3.25}]$**. Using the ratio **$\Delta K_{eff,\ \sigma}/\Delta K_{eff,\ \varepsilon}$** calculated from Newman's closure function, this prediction error is plotted in Figure 2 as a function of **σ_{max}** and **R**.

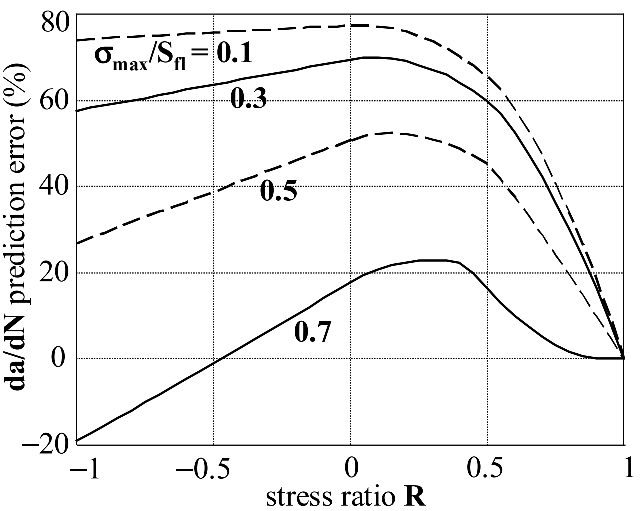

Figure 2. Non-conservative **da/dN** prediction errors for ***plane strain*** calculations based on ***plane stress*** data, according to Newman's closure function.

Therefore, since it is the thickness **t** the parameter that controls the stress state, one could expect the fatigue life of thin (plane stress dominated) structures to be ***much*** higher than the life of thick (plane strain dominated) ones, when both work under the same (initial) **ΔK** and **R**. One could also expect intermediate thickness structures, where the stress state is not plane stress nor plane strain dominated, to have **$1 < \alpha < 1/(1 - 2\nu)$** and a transitional behavior. Moreover, this transition can occur in the same piece, if the crack starts under plane strain and progressively grows toward a plane stress dominated state. However, unlike the thickness effect on fracture toughness, the dominant stress state usually is ***not*** object of much concern in fatigue design, but it certainly deserves a closer experimental verification.

Some other results are worth mentioning. When examining Ti6Al4V by the electropotential method, Shih and Wei [7] also discovered that crack closure depends on **R** and on **K_{max}** too, which is in agreement with Dugdale's theory [8]. In addition, in that titanium alloy no crack closure was found for **$R > 0.3$**. According to Shih and Wei, neither the influence of **R** on the crack propagation nor the retardation effects can be ***completely*** explained by crack closure.

Bachmann and Munz [9] also conducted crack closure measurements on Ti6Al4V, using an extensometer. However, unlike Shih and Wei, they were not able to discover any influence of **K_{max}** on crack closure behavior, which in turn would seem to confirm Elber's results.

In summary, the equations presented in this section are derived from experimental data or finite-element predictions for ***constant-amplitude*** fatigue tests. As such they can account for closure effects in ***constant*** amplitude fatigue data (by collapsing **da/dN** vs. **ΔK** curves for multiple **R** values), but they ***cannot*** account for stress interaction effects such as growth rate retardation or acceleration ***after*** overloads or underloads. To recognize load interaction effects, it is in general necessary to compute the overload-induced plastic zone size and compare it with the (embedded) current plastic zone. The next section presents analytical models to account for such load interaction effects.

LOAD INTERACTION MODELS

The above-mentioned results show the importance of the crack closure concept, and most load ***interaction*** models are, directly or indirectly, based on Elber's original crack closure idea. This implicates in the supposition that the main fatigue crack growth retardation mechanism after an overload is caused by plasticity induced crack closure. This mechanism would cause the opening load **K_{op}** to ***increase*** due to the overload inflated plastic zone ahead of the crack tip, ***reducing*** **ΔK_{eff}** and delaying subsequent crack growth.

In fact, most models that have been developed to account for load interaction effects in fatigue crack propagation are based on Elber's crack closure idea. In these models, the retardation mechanism is considered to act only within the overload-induced plastic zone situated in front of the crack tip. The size of this overload plastic zone being (considerably) greater than the size of the plastic zone induced by subsequent load cycles, an increased compressive stress state would be set up inside that region. This state would be then the main contributing factor for reducing the crack propagation rate under smaller succeeding loads.

For calculation purposes, one way of estimating the overload-induced plastic zone size $\mathbf{Z_{ol}}$ is using Irwin's expressions for plane stress and plane strain

$$(Z_{ol})_{\text{plane stress}} = \frac{1}{2\pi}\left(\frac{K_{ol}}{S_Y}\right)^2 \quad (7)$$

$$(Z_{ol})_{\text{plane strain}} = \frac{1}{6\pi}\left(\frac{K_{ol}}{S_Y}\right)^2 \quad (8)$$

where $\mathbf{K_{ol}}$ is the maximum stress intensity factor at the overload and $\mathbf{S_Y}$ is the material tensile yield strength. A more general expression for the plastic zone size proposed by Newman [10] is given by

$$Z_{ol} = \frac{\pi}{8}\left(\frac{K_{ol}}{\alpha_p S_Y}\right)^2 \quad (9)$$

where the constraint factor α_p is defined as a function of the specimen (plate) thickness **t**,

$$\alpha_p = 1.15 + 1.4 \cdot e^{-0.95\left(K_{ol}/S_Y\sqrt{t}\right)^{1.5}} \quad (10)$$

However, based on the ***maximum*** size of the plastic zone predicted by the HRR field, which is approximately the same both in plane stress and in plane strain (being however in the crack plane direction ahead of the crack tip in plane stress but not in plane strain [11]), some prefer to use equation (7) for both stress states.

Topper et al. [12], when performing experiments on SAE 1045 steel, recently discovered that high overload stress levels cause drastic reductions in the crack closure level and a large increase in subsequent crack growth rate and damage, confirming Newman's prediction. Their results implied that Elber's original crack closure concept is only applicable for nominal stress levels below half the material's tensile yielding strength $\mathbf{S_Y}$. For overloads beyond $\mathbf{S_Y/2}$ (especially for those close to $\mathbf{S_Y}$), it was found that the crack opening stress σ_{op} is significantly reduced, resulting in reduction in retardation of the crack growth after the overload. They proposed an equation for σ_{op} that depends not only on **R**, but also on the maximum overload stress σ_{ol} and $\mathbf{S_Y}$

$$\sigma_{op} = \alpha_1 \cdot \sigma_{ol}\left[1-\left(\frac{\sigma_{ol}}{S_Y}\right)^2\right] + \alpha_2 \cdot R \cdot \sigma_{ol} \quad (11)$$

where α_1 and α_2 are empirical constants. They also found that compressive underloads near the material's compressive yielding strength can cause crack acceleration due to flattening of the fracture surface asperity. Such flattening reduces the roughness-induced closure effect, decreasing as well the crack opening stress.

Perhaps the best-known fatigue crack growth retardation models are those developed by Wheeler [13] and by Willenborg [14]. Both use the same idea to decide whether the crack is retarded or not: under variable loading, fatigue crack growth retardation is predicted when the plastic zone of the **i**-th load event $\mathbf{Z_i}$ is embedded within the plastic zone $\mathbf{Z_{ol}}$ induced by a previous overload, and it is assumed dependent on the distance from the border of $\mathbf{Z_{ol}}$ to the tip of the **i**-th crack plastic zone $\mathbf{Z_i}$, see Figure 3.

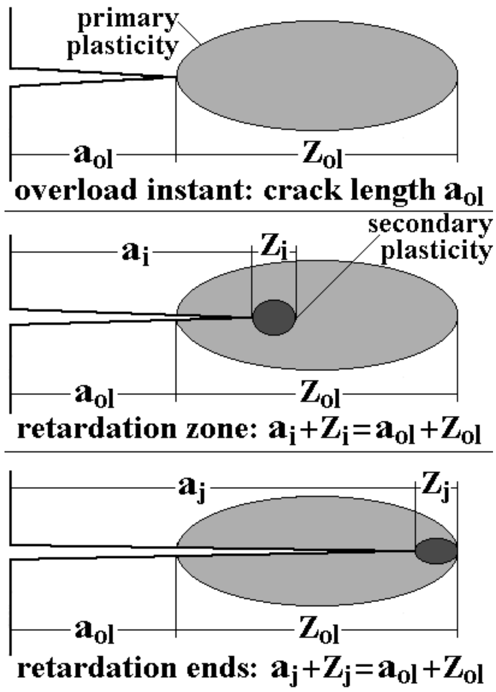

Figure 3. Yield zone crack growth retardation region used by Wheeler and by Willenborg.

In that figure, $\mathbf{a_{ol}}$ is the size of the crack when the overload occurs, and $\mathbf{a_i}$ is the (larger) crack size at the **i**-th load event, which occurs after the overload. According to both the Wheeler and the Willenborg models, load interaction effects would end when $\mathbf{a_{ol}} + \mathbf{Z_{ol}} = \mathbf{a_i} + \mathbf{Z_i}$. Moreover, the magnitude of the retardation effect would be maximum at the very first cycle after the overload, and it would steadily decrease as the crack progressively grew through the overload plastic zone.

This assumption may be mathematically convenient, but it is hard to physically justify. If the crack must enter the overload inflated plastic zone to be retarded, it does not seem reasonable to assume that the maximum retardation effect occurs in the very first cycle after it, when the crack barely crossed the $\mathbf{Z_{ol}}$ frontier. In fact, von Euw et al. [15] obtained experimental results under ***plane stress*** conditions that support this view.

The main difference between the Wheeler and Willenborg models is that the latter quantifies the retardation effect by reducing $\mathbf{K_{max}}$ and $\mathbf{K_{min}}$ acting on the crack tip, while Wheeler accounts it by direct reduction of the crack propagation rate **da/dN**. Based on this and other differences, the load interaction models presented in this work are divided into 4 categories, as follows.

da/dN INTERACTION MODELS – The **da/dN** interaction models use retardation functions to directly reduce the calculated crack propagation rate **da/dN**. ***Wheeler*** is the most popular of such models [13]. He introduced a crack-growth reduction factor, $\mathbf{C_r}$, bounded by zero and unity, which is calculated for each cycle to predict retardation as long as the current plastic zone is contained within a previously overload-induced plastic zone (this is the fundamental assumption of the yield zone models). The retardation is maximum just after the overload, and stops when the border of $\mathbf{Z_i}$ touches the border of $\mathbf{Z_{ol}}$, see Figure 3.

Therefore, if $\mathbf{a_{ol}}$ and $\mathbf{a_i}$ are the crack sizes at the instant of the overload and at the (later) **i**-th cycle, and $\mathbf{(da/dN)_{ret,i}}$ and $\mathbf{(da/dN)_i}$ are the retarded and the corresponding non-retarded crack growth rate (at which the crack would be growing in the **i**-th cycle if the overload had not occurred), then, according to Wheeler

$$\left(\frac{da}{dN}\right)_{ret,i} = \left(\frac{da}{dN}\right)_i \cdot C_r = \left(\frac{da}{dN}\right)_i \cdot \left(\frac{Z_i}{Z_{ol} + a_{ol} - a_i}\right)^{\beta} \quad (12)$$

where $\mathbf{a_i} + \mathbf{Z_i} < \mathbf{a_{ol}} + \mathbf{Z_{ol}}$, and $\boldsymbol{\beta}$ is an experimentally adjustable constant, obtained by selecting the closest match among predicted crack growth curves (using several $\boldsymbol{\beta}$-values) with an experimental curve measured under spectrum loading.

Wheeler found experimentally that the shaping exponent, $\boldsymbol{\beta}$, was material dependent, having values of **1.43** for a steel and **3.4** for the titanium alloy Ti-6Al-4V. Broek [2] suggests that other typical values for $\boldsymbol{\beta}$ are between **0** and **2**. However, flight-by-flight crack propagation tests performed by Sippel et al. [16] have shown that the exponent $\boldsymbol{\beta}$ is dependent not only on the material, but also on the crack shape, on the stress level, as well as on the type of load spectrum. Therefore, the designer should be aware that life predictions based on limited amounts of supporting test data, or for load spectra radically different from those for which the exponent $\boldsymbol{\beta}$ was derived, can lead to inaccurate and ***non-conservative*** results.

Finney [17] found experimentally that the calibration $\boldsymbol{\beta}$-value depends on the maximum overload stress $\boldsymbol{\sigma_{ol}}$ in the spectrum and on the crack shape parameter **Q** (**Q = 1** for through cracks and $\mathbf{Q = 1+1.464 \cdot [a/c]^{1.65}}$ for surface cracks with depth **a** and width **2c**). The $\boldsymbol{\beta}$-value tends to vary with these parameters in the same way as does the stress intensity factor **K**, i.e., it increases with the maximum overload stress $\boldsymbol{\sigma_{ol}}$ and decreases with the crack shape parameter **Q**.

According to Finney, increasing $\boldsymbol{\sigma_{ol}}$ stress levels would result in ***increased*** retardation, contradicting Newman's results for constant amplitude closure. Finney proposed that the exponent $\boldsymbol{\beta}$ can be represented as a function of the parameter $\boldsymbol{\sigma_{ol}/\sqrt{Q}}$. A typical relation, based on Finney's experimental results, is proposed as

$$\beta = \sqrt{B_1 \frac{\sigma_{ol}}{\sqrt{Q}} - B_2} \quad (13)$$

where $\mathbf{B_1}$ and $\mathbf{B_2}$ are experimentally adjustable positive constants. The penalty of this approach is the need for additional testing to adjust these constants.

In summary, the selection of proper values for the Wheeler exponent $\boldsymbol{\beta}$ can yield reasonable crack-growth predictions when the (complex) loads have spectra similar to the tests used to obtain $\boldsymbol{\beta}$. However, the classical Wheeler model cannot predict the phenomenon of crack ***arrest***. As $\mathbf{Z_i \approx (K_{max}/S_Y)^2}$, the lowest value of the predicted retardation factor happens immediately after the overload, and it is equal to $\mathbf{(K_{max}/K_{ol})^{2\beta}}$, where $\mathbf{K_{max}}$ is the maximum stress intensity factor in the cycle just after the overload, and $\mathbf{K_{ol}}$ is the maximum stress intensity factor at the overload. Therefore, the phenomenology of the load interaction problem is not completely reproducible by the Wheeler model, since its retardation factor is always different than zero. To consider crack arrest, a modification of the Wheeler original model is presented next.

ΔK INTERACTION MODELS – The **ΔK** interaction models use retardation functions to directly reduce the value of the stress intensity range **ΔK**. Meggiolaro and Castro [18] proposed a simple but effective modification to the original Wheeler model in order to predict both crack retardation and arrest. This approach, called the ***Modified Wheeler*** model, uses a Wheeler-like parameter to multiply **ΔK** instead of **da/dN** after the overload

$$\Delta K_{ret}(a_i) = \Delta K(a_i) \cdot \left(\frac{Z_i}{Z_{ol} + a_{ol} - a_i}\right)^{\gamma} \quad (14)$$

where $\Delta K_{ret}(a_i)$ and $\Delta K(a_i)$ are the values of the stress intensity ranges that would be acting at a_i with and without retardation due to the overload, $a_i + Z_i$ is smaller than $a_{ol} + Z_{ol}$, and γ is an experimentally adjustable constant, in general different from the original Wheeler model exponent β.

This simple modification can be used with ***any*** of the propagation rules that recognize ΔK_{th} to predict both retardation and ***arrest*** of fatigue cracks after an overload, the arrest occurring if $\Delta K_{ret}(a_i) \leq \Delta K_{th}$ (there are more than thirty such **da/dN** vs. ΔK rules in the **ViDa** software database [3], but using its equation interpreter any other rule can be typed in by the user). In addition to the retarded stress intensity range ΔK_{ret}, the retarded stress ratio R_{ret} can also be calculated as

$$R_{ret}(a_i) = 1 - \Delta K_{ret}(a_i) / K_{max}(a_i) \tag{15}$$

where $K_{max}(a_i)$ is the maximum load at the **i**-th cycle.

However, the Modified Wheeler model cannot predict the ***reduction*** of the retardation effects due to ***underloads*** subsequent to overload cycles, a phenomenon also referred to as fatigue crack acceleration [1]. An underload cycle occurs when its minimum value K_{min} is significantly smaller than the corresponding values of the previous or the subsequent cycles.

Chang et al. [19] proposed the concept of an effective overload plastic zone to model crack acceleration. In Chang's crack acceleration concept, the overload plastic zone Z_{ol} is reduced to $(Z_{ol})_{ul}$ after a compressive underload, reducing the crack retardation effects by increasing the retardation parameter from equations (12) and (14). Chang's acceleration concept was originally developed for the Willenborg model, considering that the compressive underload ***immediately*** follows the overload, but it may be adapted to the Wheeler and Modified Wheeler models using

$$(Z_{ol})_{ul} = (1 + \overline{R}_{ul}) \cdot Z_{ol}, \text{ where}$$
$$\overline{R}_{ul} = \begin{cases} 0, & \text{if } R_{ul} \geq 0 \\ R_{ul}, & \text{if } R^- < R_{ul} < 0 \\ R^-, & \text{if } R_{ul} \leq R^- \end{cases} \tag{16}$$

where R_{ul} is the underload stress ratio σ_{ul}/σ_{ol}, σ_{ul} being the lowest underload stress **after** the most recent overload σ_{ol}, and R^- is a cutoff value for negative stress ratios (typically $R^- = -0.5$, where $-1 < R^- < 0$).

Using this idea to calculate the (increased) value of ΔK_{ret}, replacing the overload plastic zone Z_{ol} by its reduced value $(Z_{ol})_{ul}$ in the retardation model, an extension of the Modified Wheeler model, called ***Generalized Wheeler***, is proposed here

$$\Delta K_{ret} = \Delta K \cdot \left(\frac{Z_i}{(1 + \alpha_{ul} \overline{R}_{ul}) Z_{ol} + a_{ol} - a_i} \right)^{\gamma} \tag{17}$$

where ΔK_{ret} is the retarded stress intensity range, $\overline{R}_{ul}$ is defined in equation (16), γ is the Modified Wheeler exponent, and the adjustable parameter α_{ul} can be used to multiply $\overline{R}_{ul}$ to better model the influence of underload stresses on crack acceleration.

This proposed model recognizes crack retardation and arrest due to overloads, and also crack acceleration (reduction in retardation) due to underloads. Another advantage of the Generalized Wheeler model is that it can be applied to ***any*** **da/dN** equation (preferably to one that recognizes ΔK_{th} to also model crack ***arrest***), in contrast with the Willenborg model, which can only be applied to **da/dN** equations that explicitly model the stress ratio **R**, as explained below.

Before leaving this section, it is worth mentioning that these retardation functions can also be based on Newman's closure function **f** in equations (3-4) to consider the stress state effect, through $\Delta K_{eff} = [(1-f)/(1-R)]\, \Delta K_{ret}$. However, one should be careful not to use Newman's approach with **da/dN** fatigue crack propagation rules that already include the effects of **f** or **R**.

R_{eff} INTERACTION MODELS – The R_{eff} load interaction models account for retardation effects by reducing both the maximum and the minimum stress intensity factors acting on the crack tip. The best-known effective stress ratio R_{eff} model is the ***Willenborg*** model [14]. As in the Wheeler model, the retardation for a given applied cycle depends on the loading and on the extent of crack growth into the overload plastic zone. Willenborg et al. assumed that the maximum stress intensity factor K_{max} occurring at the current crack length a_i is reduced by a residual stress intensity K_{RW} calculated, more or less arbitrarily, from the difference between the stress intensity required to produce a plastic zone that would reach the overload zone border (distant $Z_{ol} + a_{ol} - a_i$ from the current crack tip) and the current maximum applied stress intensity K_{max}

$$K_{RW} = K_{ol} \sqrt{(Z_{ol} + a_{ol} - a_i)/Z_{ol}} - K_{max} \tag{18}$$

where K_{ol} is the maximum stress intensity of the overload, Z_{ol} is the overload plastic zone size, and a_{ol} is the crack size at the occurrence of the overload (see Figure 3).

Willenborg et al. assumed that both stress intensity factors K_{max} and K_{min} at the current **i**-th cycle are reduced by K_{RW}. Thus, since the stress intensity range ΔK is unchanged by this uniform reduction, the retardation effect is only caused by the change in the effective stress ratio R_{eff} calculated by

$$\mathbf{R_{eff}} = \frac{\mathbf{K_{eff,min}}}{\mathbf{K_{eff,max}}} = \frac{\mathbf{K_{min}} - \mathbf{K_{RW}}}{\mathbf{K_{max}} - \mathbf{K_{RW}}} \tag{19}$$

As a result, all crack propagation rules that do not model explicitly the effects of the stress ratio **R** ***cannot*** be used with the Willenborg retardation model. For instance, if the Paris law is used to describe crack propagation, the Willenborg model will ***not*** predict crack retardation after overloads, since the value of $\mathbf{\Delta K}$ remains unchanged (and thus the value of **da/dN** as well). This is a limitation of the Willenborg formulation, not present in the Wheeler model.

In early calculations with the Willenborg model, if the calculated $\mathbf{R_{eff}}$ was negative, then it was considered equal to zero in the **da/dN** equation, making $\mathbf{\Delta K = K_{eff,max}}$. Recent evidence, however, supports the use of negative values of $\mathbf{R_{eff}}$, as long as a **da/dN** equation with a negative stress ratio cut-off is used.

Another problem in the original Willenborg model is the prediction that $\mathbf{K_{eff,max} = 0}$ (and therefore crack ***arrest***) immediately after an overload if $\mathbf{K_{ol} \geq 2\ K_{max}}$. That is, if the overload is at least twice as large as the following loads, Willenborg implies that the crack arrests, independently of the material properties, stress level, or load spectrum.

To account for the observations of continuing crack propagation after overloads larger than a factor of two or more, several modifications to the original Willenborg model have been proposed. Some examples of such modifications are the ***Generalized Willenborg*** (GW) model [20], the ***Modified Generalized Willenborg*** (MGW) model [21], and the ***Walker-Chang Willenborg*** (WCW) model [19]. The latter two have the advantage of accounting for reduction in retardation after a compressive underload.

However, even with all proposed modifications to improve the original Willenborg model, the assumption regarding the residual compressive stresses through the residual stress intensity $\mathbf{K_{RW}}$ is still at least very doubtful. To better model the closure effects on crack retardation, some methods ***directly*** estimate the value of the opening stress intensity factor $\mathbf{K_{op}}$, instead of indirectly accounting for its effects through arbitrary parameters such as $\mathbf{K_{RW}}$. These $\mathbf{K_{op}}$ load interaction models are presented next.

$\mathbf{K_{op}}$ INTERACTION MODELS – In the $\mathbf{K_{op}}$ models, the opening stress intensity factor $\mathbf{K_{op}}$ caused by an overload is directly computed and applied to the subsequent crack growth to account for Elber-type crack closure. Perhaps the simplest $\mathbf{K_{op}}$ model is the ***Constant Closure*** model, originally developed at Northrop for use on their classified programs [22]. This load interaction model is based on the observation that for some load spectra the closure stress does not deviate significantly from a certain stabilized value. This value is determined by assuming that the spectrum has a "controlling overload" and a "controlling underload" that occur often enough to keep the residual stresses constant, and thus the closure level constant.

In the constant closure model, the opening stress intensity factor $\mathbf{K_{op}}$ is the only empirical parameter, with typical values estimated between 30% and 50% of the maximum overload stress intensity factor. The crack opening stress $\mathbf{K_{op}}$ can also be calculated, for instance, from Newman's closure function given in equations (3-4), using the stress ratio **R** between the controlling underload and overload stresses. The value of $\mathbf{K_{op}}$, calculated for the controlling overload event, is then applied to the following (smaller) loads to compute crack growth, recognizing crack retardation and even crack arrest (if $\mathbf{K_{max} \leq K_{op}}$).

The main limitation of the Constant Closure model is that it can only be applied to loading histories with "frequent controlling overloads," because it does ***not*** model the ***decreasing*** retardation effects as the crack tip cuts through the overload plastic zone. In this model, it is assumed that a new overload zone, with primary plasticity, is formed often enough before the crack can significantly propagate through the previous plastic zone, thus not modeling secondary plasticity effects by keeping $\mathbf{K_{op}}$ constant.

To account for crack retardation due to ***both*** primary and secondary plasticity (Figure 3), the European Space Agency and the National Aerospace Laboratory, in cooperation with NASA, developed the ***DeKoning-Newman Strip Yield*** (SY) load interaction model [23]. In this model, a crack growth law is described in an incremental way, modeling crack growth attributed to increments $\mathbf{\delta K}$ in the stress intensity factor as the crack changes from closed to fully open configurations. This incremental law is then integrated ***at each cycle*** from the minimum to the maximum applied stress intensity factors $\mathbf{K_{min}}$ and $\mathbf{K_{max}}$ to find the crack growth rate **da/dN**. A detailed discussion of this model is found in [23].

There are several other load interaction models in the literature [24], but none of them has definitive advantages over the models discussed above. This is no surprise, since single equations are too simplistic to model all the several mechanisms that can induce retardation effects. Therefore, in the same way that a curve **da/dN** vs. $\mathbf{\Delta K}$ must be experimentally measured, a load interaction model must still be adjusted to experimental data to calibrate its parameters, as recommended by Broek [2].

EVALUATION OF LOAD INTERACTION MODELS

In this section, the presented load interaction models and the proposed modifications are compared with some experimental results from various load spectra. Only the DeKoning-Newman Strip Yield model is not included in this comparison, because it depends on several experimental constants not available for the considered material.

All load interaction models presented in this work have been implemented in a general-purpose fatigue design program named **ViDa**, developed to predict both initiation and propagation fatigue lives under complex loading by all classical design methods. Using the efficient numerical integration facilities available in this software, the crack propagation life of an 8-mm-thick center-cracked tensile specimen, made of a 7475-T7351 aluminum alloy, is calculated using several block loading histories (see Table 1). The calculated lives are compared to experimental tests performed by Zhang [25], who measured crack growth rates through scanning electron microscopy. These predictions have also been successfully validated through a comparison with similar calculations performed by **NASGRO**, the crack growth program developed by **NASA** [26]. However, the latter software only considers the $\mathbf{R_{eff}}$ and the $\mathbf{K_{op}}$ retardation models, and it restricts the choice of the **da/dN** expression to Forman-Newman's equation (6).

On the other hand, **ViDa**'s database includes over thirty **da/dN** equations, and accepts any other through its equation interpreter, reflecting its open philosophy in fatigue design. In this way, the user can choose for instance whether or not to use Newman's closure function **f** in crack growth. Furthermore, it includes ***all*** the load interaction models presented in this work, granting flexibility to the end-user.

For consistency purposes, the calculations presented in this section were performed selecting Forman-Newman's equation (6), computing crack growth using $\mathbf{A = 6.9 \cdot 10^{-7}}$, $\mathbf{m = 2.212}$, $\mathbf{p = 0.5}$, $\mathbf{q = 1.0}$, the same parameters used by **NASGRO**. The propagation threshold for $\mathbf{R = 0}$ is $\mathbf{\Delta K_0 = 3MPa\sqrt{m}}$, used to compute the threshold stress intensity range through equation (2).

Also, the plane-strain fracture toughness of the considered alloy is $\mathbf{K_{Ic} = 38MPa\sqrt{m}}$. A modified version of the $\mathbf{K_C}$-versus-thickness behavior proposed by Vroman [27] is used to compute the fracture toughness under the stress condition of the $\mathbf{t = 8mm}$ plate thickness,

$$\mathbf{K_C(t)/K_{Ic} = 1.0 + e^{-\left(\frac{S_Y^2 \cdot t}{2.5 \cdot K_{Ic}^2}\right)^2}} \tag{20}$$

resulting in $\mathbf{K_C = 73MPa\sqrt{m}}$. Newman's closure function **f** was used for $\mathbf{\sigma_{max}/S_{fl} = 0.3}$ and a constant plane stress/strain constraint factor $\mathbf{\alpha = 1.9}$. All models had their adjustable parameters calibrated using the first loading history (except for the Willenborg model, without parameters to be adjusted), and their comparison is made from the remaining loadings. Table 1 shows Zhang's test results and the percentage error of the predicted lives using several load interaction models.

Table 1. Percentage errors in the test lives predicted by the load interaction models.

Loading history (MPa)	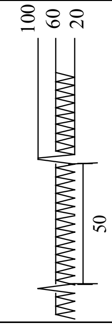	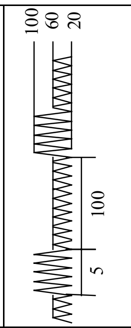	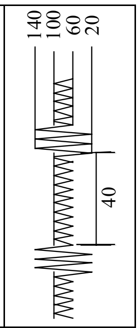
Zhang's test (cycles)	**474,240**	**409,620**	**149,890**
No Interaction	−17%	−13%	−2.3%
Wheeler	0%	+2.3%	+6.6%
Generalized Wheeler	0%	+2.3%	+6.4%
Willenborg	+293%	+185%	+44%
Generalized Willenborg	0%	+2.2%	+4.0%
Modif. Gen. Willenborg	0%	+2.6%	+42%
Constant Closure	0%	+2.4%	−60%

As expected, the Willenborg model resulted in poor predictions, since this model cannot be calibrated. The remaining models performed similarly for the second load history. However, as the maximum load increased from 100 to 140 MPa in the last history, the Modified Generalized Willenborg and the Constant Closure models showed increased errors. All Wheeler-type models and the Generalized Willenborg model resulted in the best predictions for Zhang's histories.

It should be noted that the Modified Wheeler and Generalized Wheeler models resulted in the same predictions, because the considered histories didn't include compressive underloads. Also, the (traditional) Wheeler and the Modified and Generalized Wheeler results were very similar, because Zhang's tests were performed under the second crack growth regime, which is not much influenced by the threshold $\mathbf{\Delta K_{th}}$ nor by the toughness $\mathbf{K_C}$ (in fact, under pure Paris controlled crack growth, $\mathbf{da/dN = A\Delta K^m}$, these rules become identical if $\mathbf{\gamma = \beta/m}$). Therefore, the advantages of the Modified and the Generalized Wheeler models in predicting crack arrest could not be exemplified above.

To compare the predictions of the models in the presence of underloads, a ***simulated*** underload event $\mathbf{\sigma_{ul}}$ was considered after each overload event, see Table 2. These simulated tests make sense since all models ***assume*** that crack closure is the sole mechanism which causes load interaction effects, and the overall behavior of the predictions illustrate their sensibility to the differences in load spectra.

Table 2. Comparison of life predictions in cycles for different underload stresses.

Loading history (MPa)	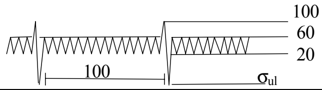			
Underload stress σ_{ul} (MPa)	**20.0**	**0.0**	**-20.0**	**-50.0**
Wheeler	497100	493700	491600	488200
Modified Wheeler	496900	493600	491350	487950
Gener. Wheeler	**496900**	**493600**	**470850**	**427750**
Gener. Willenborg	497650	494500	492350	488950
Mod.Gen.Willenb.	**499350**	**457850**	**444300**	**433000**
Constant Closure	497100	495700	494600	492350

As expected, the Generalized Wheeler and the Modified Generalized Willenborg were the only load interaction models that predicted reduction in retardation (and thus reduced life) after compressive underloads. The other models showed a slight reduction in the calculated lives in the presence of underloads, however this small change was caused only by the increased **ΔK** ***at*** (and not ***after***) the overload/underload event.

However, as it was shown in Table 1, the Modified Generalized Willenborg model ***only*** resulted in good predictions when the 100MPa overload level (used in its calibration) was maintained. Thus, the Generalized Wheeler was the only model that performed well at all overload levels, while considering crack acceleration due to underloads and crack arrest.

Finally, the Generalized Wheeler model is used to study the overload frequency dependence of fatigue crack growth (which cannot be captured by the Constant Closure model, because it does not consider secondary plasticity). Figure 4 shows the predicted fatigue lives associated with ***simulated*** loading histories with different numbers of cycles between overloads.

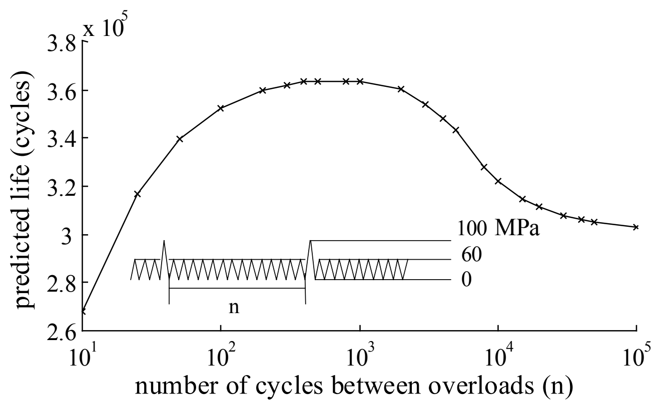

Figure 4. Generalized Wheeler life predictions for several simulated overload frequencies.

As seen in Figure 4, the maximum predicted life in this case is obtained when the overloads are separated by approximately 500 cycles (the "optimal" overload frequency). Any overload frequency other than this will lead to increasing crack growth (and thus decreased life), even if the overload is removed. In fact, if the overloads are too frequent, they become the rule instead of the exception in the loading history, decreasing the fatigue life due to their increased **ΔK**. On the other hand, if the overloads are scarce, the crack is able to completely cut through the plastic zone generated by the previous overload before the next event, reducing the retardation effects and the fatigue life. Therefore, fatigue life can be significantly ***increased*** in the presence of overloads if they're applied at an ***optimal*** frequency, which can be calculated e.g. using the **ViDa** software [3].

CONCLUSIONS

In this work, load interaction effects on fatigue crack propagation were discussed, based on the crack closure idea. Overload-induced retardation effects on the crack growth rate were evaluated using several different models, and improvements to the traditional equations were proposed to recognize crack arrest and acceleration due to compressive underloads. The models were evaluated using a general-purpose fatigue design program named **ViDa**, developed to predict both initiation and propagation fatigue lives under complex loading by all classical design methods. Using this software, the presented load interaction models and the proposed modifications were compared with experimental results on center-cracked tensile specimens for various load spectra. In particular, the proposed modifications to the Wheeler model showed a good agreement with the experimental data and a better response to varying characteristics of the loading spectra. In addition, assuming that crack closure is the only retardation mechanism, it was found that the propagation rate **da/dN** should be a strong function of the specimen thickness **t**, which controls the dominant stress-state at the crack tip. However, this thickness effect on **da/dN** has not been object of much concern in fatigue design, but it certainly deserves a closer experimental verification.

REFERENCES

[1] Suresh, S. Fatigue of Materials. Cambridge: Cambridge University Press, 1991.

[2] Broek, D. The Practical Use of Fracture Mechanics. Kluwer, 1988.

[3] Castro,J.T.P., Meggiolaro,M.A. Fatigue Design under Complex Loading (in Portuguese). Pontifical Catholic University of Rio de Janeiro, 2001.

[4] Elber, W. The Significance of Fatigue Crack Closure. ASTM STP 486, 1971.

[5] Newman, Jr., J.C. A Crack Opening Stress Equation for Fatigue Crack Growth. International Journal of Fracture 1984;24(3):R131-R135.

[6] Forman, R.G., Mettu, S.R. Behavior of Surface and Comer Cracks Subjected to Tensile and Bending Loads in Ti-6Al-4V Alloy. ASTM STP 1131, 1992:519-546.

[7] Shih, T.T., Wei, R.P. A Study of Crack Closure in Fatigue. Engineering Fracture Mechanics 1974;6:19-32.

[8] Führing, H., Seeger, T. Dugdale Crack Closure Analysis of Fatigue Cracks under Constant Amplitude Loading. Engineering Fracture Mechanics 1979;11(1).

[9] Bachmann, V., Munz, D. Crack Closure in Fatigue of a Titanium Alloy. Int. Journal of Fracture, 1975;11.

[10] Newman, Jr., J.C., Crews, Jr., J.H., Bigelow, C.A., Dawicke, D.S. Variations of a global constraint factor in cracked bodies under tension and bending loads. Constraint Effects in Fracture: Theory and Applications, ASTM STP 1244, 1995;21-42.

[11] Hutchinson, J.W. Non-Linear Fracture Mechanics. Technical University of Denmark, 1979.

[12] Topper, T.H., Varvani-Farahani, A., Dabayeh, A., Lam, T. Variable amplitude fatigue life predictions incorporating the effect of overload induced changes in crack closure. Proceedings of the Eighth International Conference on the Mechanical Behaviour of Materials, ICM8, 1999;1:116-121.

[13] Wheeler, O.E. Spectrum Loading and Crack Growth. Journal of Basic Engineering, 1972;181-186.

[14] Willenborg, J., Engle, R.M., Wood, H.A. Crack Growth Retardation Model Using an Effective Stress Concept. Air Force Flight Dynamics Laboratory, Wreight Patterson Air Force Base, TM 71-1-FBR, 1971.

[15] von Euw, E.F.G., Hertzberg, R.W., Roberts,R. Delay Effects in Fatigue Crack Propagation. ASTM STP 513, 1972;230-259.

[16] Sippel, K.O., Weisgerber, D. Flight by Flight Crack Propagation Test Results with Several Load Spectra and Comparison with Calculation According to Different Models. ICAF Symposium, Darmstadt, 1977.

[17] Finney, J.M. Sensitivity ot Fatigue Crack Growth Prediction (Using Wheeler Retardation) to Data Representation. Journal of Testing and Evaluation, 1989;17(2):75-81.

[18] Meggiolaro, M.A., Castro, J.T.P. Modelagem dos Efeitos de Sequência na Propagação de Trincas por Fadiga (in Portuguese). II Congresso Internacional de Tecnologia Metalúrgica e de Materiais, ABM, 1997.

[19] Chang, J.B., Engle, R.M., Szamossi, M. An Improved Methodology for Predicting Random Spectrum Load Interaction Effects on Fatigue Crack Growth. Proceedings of the Fifth International Conference on Fracture, Pergamon Press, New York, 1981.

[20] Gallagher. J.P. A Generalized Development of Yield Zone Models. AFFDL-TM-74-28-FBR, Wright Patterson Air Force Laboratory, 1974.

[21] Abelkis, P.R. Effect of Transport Aircraft Wing Loads Spectrum Variation on Crack Growth. Proceedings of the Effect of Load Spectrum Variables on Fatigue Crack Initiation and Propagation Conference, San Francisco, CA, ASTM STP 714, 1980;143-169.

[22] Bunch, J.O., Trammell, R.T., Tanouye, P.A. Structural life analysis methods used on the B-2 bomber. Advances in fatigue lifetime predictive techniques: 3rd Volume, A96-26758 06-39, ASTM, 1996;220-247.

[23] de Koning, A.U., ten Hoeve, H.J., Hendriksen, T.K. The description of crack growth on the basis of the strip-yield model for computation of crack opening loads, the crack tip stretch and strain rates. National Aerospace Laboratory (NLR), Report: NLR-TP-97511L, 1997.

[24] Chang, J.B., Hudson, C.M. eds. Methods and Models for Predicting Fatigue Crack Growth Under Random Loading. ASTM STP 748, 1981.

[25] Zhang, S., Doker, H., Trautmann, K., Nowack, H., Schulte, K. Exact Determination of Delta Keff and Crack Propagation Prediction for Selected Loading Sequences. Advances in Fatigue Lifetime Predictive Techniques, ASTM STP 1211, 1993;2:54-71.

[26] Forman, R.G., Shivakumar, V., Mettu, S.R., Newman, J.C., Jr. Fatigue Crack Growth Computer Program NASGRO Version 3.0. Reference Manual, NASA JSC-22267B, August 2000.

[27] Vroman, G.A. Material Thickness Effect on Critical Stress Intensity. Monograph #106, TRW Space and Technology Group, 1983.